Chemical Engineering Journal 340 (2018) 32–41

Contents lists available at ScienceDirect

Chemical Engineering Journal

journal homepage: www.elsevier.com/locate/cej

Polyethyleneimine coated nanogels for the intracellular delivery of RNase A for cancer therapy

Neda Kordalivand[a], Dandan Li[a], Nataliia Beztsinna[a], Javier Sastre Torano[b], Enrico Mastrobattista[a], Cornelus F. van Nostrum[a], Wim E. Hennink[a,*], Tina Vermonden[a]

[a] Department of Pharmaceutics, Utrecht Institute for Pharmaceutical Sciences, Utrecht University, Utrecht, The Netherlands
[b] Chemical Biology and Drug Discovery, Utrecht Institute for Pharmaceutical Sciences, Utrecht University, Utrecht, The Netherlands

ARTICLE INFO

Keywords:
Dextran
Nanogels
Ribonuclease A
Polyethyleneimine
Triggered release
Apoptosis
Drug delivery

ABSTRACT

The aim of this study was to deliver ribonuclease A (RNase A) intracellularly using dextran nanogels for cancer treatment. To this end, positively charged RNase A was electrostatically loaded in anionic dextran nanogels with an average size of 205 nm, which were prepared by an inverse mini-emulsion technique. To chemically immobilize the loaded protein in the nanogels and prevent its unwanted release in the extracellular environment, the protein was covalently linked to the nanogel network via disulfide bonds, which are cleavable in the reductive cytosolic environment. A high loading efficiency and loading content of RNase A (75% and 20%, respectively) were obtained. Coating of the nanogels with the cationic polymer polyethyleneimine reversed the zeta potential of nanogels from −31.6 mV to +7.6 mV. The nanogels showed a fast and triggered release of RNase in the presence of glutathione. Negatively charged RNase A loaded nanogels did not show cytotoxicity, likely due to their limited cellular uptake. In contrast, PEI coated RNase A loaded nanogels showed high uptake by MDA-MB 231 breast cancer cells and exhibited a concentration-dependent cytotoxic effect by apoptosis. The results demonstrate that PEI coated nanogels are promising nano-carriers for intracellular protein delivery, encouraging further evaluation of this formulation in preclinical models.

1. Introduction

Due to the remarkable advances in molecular biology and biotechnology, proteins and peptides have raised tremendous attention as potent therapeutics to combat a large number of diseases [1–3]. Although most pharmaceutical proteins act on receptors present on cell membranes, many proteins also have their target inside the cell and they must be translocated into the cytoplasm or organelles to exert their therapeutic effects. Research towards proteins acting intracellularly are underrepresented in literature because of their poor transport over cellular membranes [4,5]. Despite their high therapeutic potential, protein-based drugs have intrinsic drawbacks hampering their pharmaceutical applications. These encompasses their chemical and physical instability, degradation due to proteases and, for proteins that have their targets intracellularly, limitations to be transported across the cell membrane [6,7].

Among different intracellular protein delivery strategies, microinjection and electroporation as physical approaches have been investigated *in vitro* in recent decades [8–10]. However, these technologies are associated with adverse effects resulting from high voltage pulses [11]. As delivery vectors, cell penetrating peptides (CPPs) have shown remarkable results to improve the permeability of cell membranes for hydrophilic macromolecular biotherapeutics [12–15]. Nevertheless, CPPs suffer from poor cell and tissue specificity and short half-life [16]. As a delivery strategy, incorporation of proteins and peptides into nanocarriers is a promising approach to improve their limited cytoplasmic delivery [17–20]. These nanocarrier systems protect the encapsulated therapeutics from physical, chemical and enzymatic degradation before reaching their target tissue and subsequently they facilitate intracellular delivery [21]. Moreover, the use of pharmaceutical nanocarriers reduces the need for multiple high dose administrations, resulting in less undesired side effects and improved patient compliance [22].

Nano-sized hydrogel particles (or nanogels), composed of hydrophilic polymeric networks, are attractive vehicles for the delivery of biotherapeutics [23–28]. Due to their high water content, high loading capacity and tunable network properties, nanogels are attractive carriers for sensitive therapeutic biomolecules such as proteins, peptides and nucleic acids. Their release kinetics can be tailored by the chemical composition of the gels and cross-link density [29,30]. Network

* Corresponding author.
E-mail address: w.e.hennink@uu.nl (W.E. Hennink).

https://doi.org/10.1016/j.cej.2017.12.071

Available online 15 December 2017

formation in nanogels can be accomplished, just as in classical macroscopic hydrogels, via physical or chemical crosslinking methods [31–33]. By controlling the hydrolytic degradation kinetics, sustained release of therapeutics from biodegradable nanogels can be achieved [34]. Importantly, triggered release can be obtained intracellularly in e.g. redox-sensitive or pH sensitive nanogels, which are susceptible to physiological differences between the intra and extracellular environment and release their content in response to these differences [35–40].

Ribonucleases (RNases) are enzymes that catalyze the hydrolytic cleavage of RNA and they play a key role in cell homeostasis [41,42] and also have potential for cancer therapy [43,44]. RNase A, a member of the ribonuclease superfamily has shown cytotoxicity against cancer cells [45,46]. However, as a result of rapid renal filtration of this small enzyme (half-life < 5 min) [47], multiple administrations of high doses of RNase A are essential to reach the required concentration in tumors, which primarily leads to accumulation of this protein in the kidneys. Local administration of protein in tumors reduces the side effects but the therapeutic efficacy remains poor due to insufficient permeability for cell membranes [48,49]. Hence, the development of an effective delivery system that stabilizes the administered RNase A and promotes the cellular association and internalization is highly desirable [50–52]. Park et al. incorporated RNase A into self-assembled heparin-Pluronic (HP) nanogels to protect the protein against degradation and enhance the intracellular delivery of the enzyme. HP nanogels loaded with RNase A were efficiently taken up by HeLa cells and induced cytotoxicity in an RNase A concentration-dependent manner [50]. However, the electrostatically immobilized protein showed unwanted release in the circulation before reaching its action site inside cells.

In the current work, we have developed a dextran-based nanogel loaded with RNase A that is stable in the extracellular environment, but that releases its payload in the cell after being internalized. To this end, RNase A, a positively charged protein, was reacted with Traut's reagent to yield thiol groups and this modified protein was subsequently loaded in anionic dextran-based nanogels exploiting electrostatic interactions between the hydrogel network and the protein. To stabilize the electrostatically loaded protein in the nanogels, the modified RNase A was covalently immobilized onto the nanogel network via disulfide bonds, which are stable in the extracellular space but cleaved in the cytosolic reducing environment. Furthermore, to trigger the cellular uptake of these anionic nanoparticles, we reversed the particle surface charge by their coating with polyethyleneimine (PEI). We evaluated the cytotoxic effect of PEI coated RNase A loaded nanogels in a breast cancer cell line and the mechanism of cell death was investigated

2. Materials and methods

2.1. Materials

Dextran (from Leuconostoc ssp.) with Mw = 40.000, glycidyl methacrylate (GMA) and hydroxyethyl methacrylate (HEMA) were purchased from Fluka. Methacrylate-derivatized dextran (dex-MA) with degrees of substitution of 8 (DS, i.e. number of MA groups per 100 glucopyranose units) was synthesized as described by van Dijk-Wolthuis et al. [53,54]. Sodium methacrylate, glutathione, and light mineral oil were obtained from Sigma (USA). ABIL EM 90 and Irgacure 2959 were purchased from Goldschmidt (Essen, Germany) and Ciba Specialty Chemicals, respectively. Branched polyethyleneimine, Mw 10,000 was purchased from Polysciences Inc. Acetone, acetonitrile, dimethyl sulfoxide, n-hexane and trifluoroacetic acid (TFA) were obtained from Biosolve (The Netherlands). Potassium persulfate and sodium bisulfite were obtained from Sigma and Fisher Scientific (Geel, Belgium), respectively. *N*-2-hydroxyethylpiperazine-*N'*-2-ethanesulfonic acid (HEPES) was purchased from Acros Chimica (Geel, Belgium). Ribonuclease A (RNase A, Type XII-A, ≥90% (SDS-PAGE)) was purchased from Sigma-Aldrich (USA). Phosphate buffer saline (Na^+ 163.9 mM, Cl^- 140.3 mM, HPO_4^{2-} 8.7 mM, $H_2PO_4^-$ 1.8 mM, pH 7.4) was purchased from Braun (Germany). Alexa Fluor® 488 and Alexa Fluor® 647 fluorescent dyes were purchased from Invitrogen (Eugene, Oregon, USA). CellEvent™ Caspase-3/7 Green Detection Reagent was purchased from Thermo Fisher Scientific. *N*-(4-(2-(pyridine-2-yldisulfanyl)ethyl)-amidobutyl) methacrylamide as a bioreducible linker was synthesized as described previously [35].

2.2. Preparation of anionic nanogels

Negatively charged nanogels were prepared using the inverse mini-emulsion technique as described by Raemdonck et al. [24] with some modifications. In short, a solution of 1 M sodium methacrylate (SMA) was prepared in HEPES buffer (1 M, pH 7.4). To tune the charge density and crosslink density of nanogels, 100 mg dex-MA (DS 8) was dissolved in 50–250 µl of 1 M sodium methacrylate solution. The final volume of the different samples was kept constant (315 µl) by adding HEPES buffer. Subsequently, 65 µl Irgacure dissolved in water (10 mg/ml) was added to the solution. This aqueous phase was emulsified in 5 ml external phase of mineral oil also containing 10% (v/v) ABIL EM 90 followed by 4 min of sonication (Tip sonicator, amplitude 25%) in an ice bath. Crosslinking was carried out by photopolymerization of the methacrylate groups through two UV irradiations (900 s, 940 mW cm^{-2}, Bluepoint UV source, Hönle UV technology). The emulsion was briefly vortexed (15 s) before the second UV irradiation. The resulting nanogels were centrifuged (3000*g*, 3 min, 4 °C) and washed once with cooled acetone and 4 times with cooled acetone/n-hexane (1.5/1 (v/v)) to remove the mineral oil and surfactant. Finally, the obtained pellets were resuspended in 5 ml reverse osmosis water and lyophilized by freeze-drying overnight. Furthermore, neutral nanogels as control were prepared by adding an equal molar amount of HEMA (instead of sodium methacrylate) as a non-charged monomer. In addition, to prepare the linker containing nanogels, 20 mg of *N*-(4-(2-(pyridine-2-yldisulfanyl) ethyl)-amidobutyl) methacrylamide synthesized as described [35] (100 mg/ml in DMSO) was added to the aqueous phase.

2.3. Preparation of anionic dextran microgels

Anionic dextran microgels were prepared in all-aqueous solution method as developed by Stenekes et al. [55] with some modifications. In short, a water-in-water emulsion of two aqueous solutions of methacrylated dextran (40% (w/w)) and PEG (40% (w/w)) was obtained by vigorous mixing for 2 min under a nitrogen atmosphere. To introduce charge into the microgels, methacrylic acid (300, 500 and 800 µmol) was added to the system. Then, the emulsified system was allowed to stabilize for 15 min. Chemically cross-linked microspheres were formed by radical polymerization by addition of potassium persulfate (50 mg/ml) and sodium bisulfite (50 mg/ml) as an initiator and catalyst, respectively and the emulsion was subsequently incubated overnight at room temperature. Finally, the microgels were purified with reverse osmosis water through three centrifugation/washing steps and subsequently lyophilized.

2.4. Labeling of RNase A, PEI and nanogels

Labeling of RNase A with Alexa Fluor™ 488 NHS Ester (succinimidyl ester) was performed according to the manufacturer's instructions. The NHS activated dye was coupled to the primary amines of the protein. In short, 10 mg of RNase A was dissolved in 1 ml of 0.1 M sodium bicarbonate buffer pH 8.3. Next, 50 µl of the amine-reactive dye (10 mg/ml in DMSO) was added to the protein solution. The reaction mixture was incubated for 1 h at room temperature with continuous stirring, followed by purification using PD 10 column chromatography and the labeled RNase A was obtained after freeze drying.

To label the nanogels, 4.2 mg of 2-aminoethyl methacrylate was added to the solution of dex-MA prior to particle formation. Next, 10 mg of freeze dried nanogels was dispersed in 0.5 ml DMSO and 10 µl

of the Alexa Fluor™ 647 NHS ester dye was added and the mixture was stirred at room temperature overnight. The labeled nanogels were purified by centrifugation and recovered after freeze drying.

The primary amine groups of PEI were reacted with NHS ester of Alexa Fluor™ 488 NHS dye. In brief, 20 mg of PEI was dissolved in 1 ml of 0.1 M sodium bicarbonate buffer pH 8.3. Then, 20 µl of the dye (1 mg/ml dissolved in DMSO) was added to the polymer solution. After 1 h incubation at room temperature, the mixture was purified by PD 10 column chromatography and the labeled polymer was obtained after freeze drying.

2.5. Nanogels and microgels characterization

The nanogels were dispersed in 10 mM HEPES buffer pH 7.4 and the average size and size distribution were measured using dynamic light scattering (DLS, Malvern ALV/CGS-3 Goniometer, Malvern, UK) at 25 °C at an angle of 90° (Z-average), equipped with Dispersion Technology Software (DTS). A laser light-blocking technique (AccuSizer 780, PSS-Nicomp, Santa Barbara, CA, USA) was used to measure the particle size and size distribution of microgels. The zeta-potential of nanogels and microgels both suspended in HEPES buffer (10 mM, pH 7.4) was determined by Zetasizer Nano-Z (Malvern Instrument Ltd.).

2.6. Absorption of RNase A in the anionic microgels

Physical absorption of RNase A into the negatively charged dex-MA-co-MA microgels was visualized by confocal microscopy. The anionic microgels (2 mg/ml) dispersed in low ionic strength buffer (20 mM HEPES, pH 7.4) were incubated with labeled RNase A (see Section 2.4) 1 mg/ml in HEPES buffer, 20 mM, pH 7.4). The mixture was kept at room temperature for 2 h. Then, the unbound protein was removed by centrifugation (30 min, 15,000 rpm) and the particles were re-dispersed in HEPES buffer (20 mM, pH 7.4). Confocal images of microgels were taken using a confocal scanning laser microscope (CLSM, Confocal Leica SPE-II, Leica Microsystems, Wetzlar, Germany).

2.7. Determination of the linker content of the nanogels

The amount of copolymerized linker (*N*-(4-(2-(pyridine-2-yldisulfanyl)ethyl)-amidobutyl) methacrylamide) in the obtained nanogels was determined by RP-HPLC. Dex-MA nanogels prepared as described in Section 2.2 (10 mg) were dispersed in 1 ml of dithiothreitol 10 mM dissolved in water (or buffer? Which?) and incubated for 2 h at 37 °C to cleave the disulfide bonds. After centrifugation of the nanogels (1 h, 15,000 rpm), 10 µl of the supernatant was injected onto an RP-18 column to quantify the concentration of 2-mercaptopyridine that was cleaved and released from the linker containing nanogels. A gradient was run from the starting composition, acetonitrile/H_2O, (10/90%), to acetonitrile/H_2O, (50/50%) in 10 min. The flow rate of the mobile phase was 1 ml/min and detection was done at 280 nm. The chromatograms were analyzed by Empower software and the calibration curve of 2-mercaptopyridine was linear between 10 and 100 µg/ml.

2.8. Modification of RNase A with 2-Iminothiolane (Traut's Reagent)

Modification of RNase A with 2-iminothiolane (Traut's Reagent), which reacts with primary amines to introduce sulfhydryl groups in proteins was performed as described previously [56]. In brief, 25 mg RNase A was dissolved in 1.25 ml phosphate buffer (pH 8, containing 4 mM EDTA), followed by the addition of a 10-fold molar excess of Traut's reagent (2.5 mg) in 1.25 ml of the same phosphate buffer. After stirring for 2 h at room temperature, the modified protein was purified by size-exclusion chromatography on a PD-10 column to remove the unreacted 2-iminothiolane and the purified modified protein was subsequently lyophilized. Ellman's reaction was performed to determine the number of free sulfhydryl groups [57]. UPLC analysis of modified protein was performed on a Waters ACQUITY UPLC® system using an ACQUITY BEH 300 C18 column (1.7 µm, 2.1 mm × 50 mm). Solvent mixtures consisting of 5% ACN/95% H_2O/0.1% (TFA) and 100% ACN/0.1% TFA were used as eluent A and B, respectively. A gradient was run from 0 to 60% B in 7 min with a flow rate of 0.25 ml/min. Mass spectra of native and modified RNase A were measured by direct infusion into a Bruker (Bremen, Germany) ESI- time-of-flight mass spectrometer.

Table 1
Characterization of charged Dex-MA-co-MA nanogels. Mean values with corresponding standard deviations (n = 3) are shown. Dex-MA with a degree of substitution of 8 MA side chains per 100 glucopyranose units was used.

SMA[a] (µmol)	Z_{ave} (nm)	ζ-potential (mV)	PDI[b]	Yield (%)
–	247 ± 9	−1.9	0.27 ± 0.09	74 ± 2
50	231 ± 7	−14.7 ± 0.5	0.03 ± 0.01	85 ± 3
150	238 ± 8	−17.9 ± 0.5	0.08 ± 0.02	82 ± 4
250	203 ± 9	−21.6 ± 0.6	0.11 ± 0.06	89 ± 7
350	220 ± 3	−27.3 ± 0.4	0.11 ± 0.06	92 ± 6
500	242 ± 2	−32.5 ± 0.8	0.18 ± 0.04	90 ± 6

[a] Sodium methacrylate monomer per 100 mg dex-MA.
[b] Polydispersity index measured by DLS.

Table 2
Characterization of negatively charged Dex-MA microgels. Mean values with corresponding standard deviations (n = 3) are shown. Dex-MA with a degree of substitution of 8 MA side chains per 100 glucopyranose units was used.

Initial water content (%)	MA (µmol)	ζ-potential (mV)	Particle size (µm)
60%	0	−6.6 ± 0.8	3.44 ± 2.23
60%	300	−10.7 ± 0.5	2.92 ± 1.57
60%	500	−15.0 ± 0.1	2.83 ± 1.39
60%	800	−18.8 ± 0.9	2.71 ± 1.18
75%	500	−16.6 ± 0.9	3.08 ± 1.53

2.9. RNase A enzymatic activity assay

The enzymatic activity of Traut's modified RNase A was determined by a method described by Kalnitsky et al. [58]. In brief, solutions of native RNase A (0–14 µg/ml) and modified RNase A (10 µg/ml) were prepared in 0.1 M sodium acetate buffer pH 5 and incubated at 37 °C for 8 min. Yeast RNA (10 mg/ml) was also dissolved in the same buffer (concentration 10 mg/ml) and incubated at 37 °C. Then, 250 µl of the native and modified RNase A solution were added to 250 µl of the RNA solution and the mixtures were incubated for 4 min at 37 °C. Finally, the enzymatic reaction was stopped by addition of 250 µl of a uranyl acetate/perchloric acid/H_2O (0.75%/25%/75%) solution followed by cooling on an ice bath for 5 min. After centrifugation for 10 min at 15,000 rpm, the collected supernatants were diluted 30 times with milliQ water and the absorbance at 260 nm was measured.

2.10. Covalent conjugation of modified RNase A

The Traut's modified RNase A (Section 2.8) was covalently immobilized in nanogels containing the pyridyldisulfide linker (Section 2.2). Suspensions of linker containing nanogels (2 mg/ml) and modified RNase A solution (2 mg/ml) in HEPES buffer 20 mM, pH 7.4 were prepared and purged with nitrogen for 15 min. Then, 2.5 ml of the RNase solution was added to 10 ml of nanogel dispersion and incubated for 24 h at room temperature. To remove the physically adsorbed protein from the nanogels, particles were washed 2 times with high ionic strength buffer (PBS, pH 7.4). Finally, the loaded particles were washed with water and lyophilized.

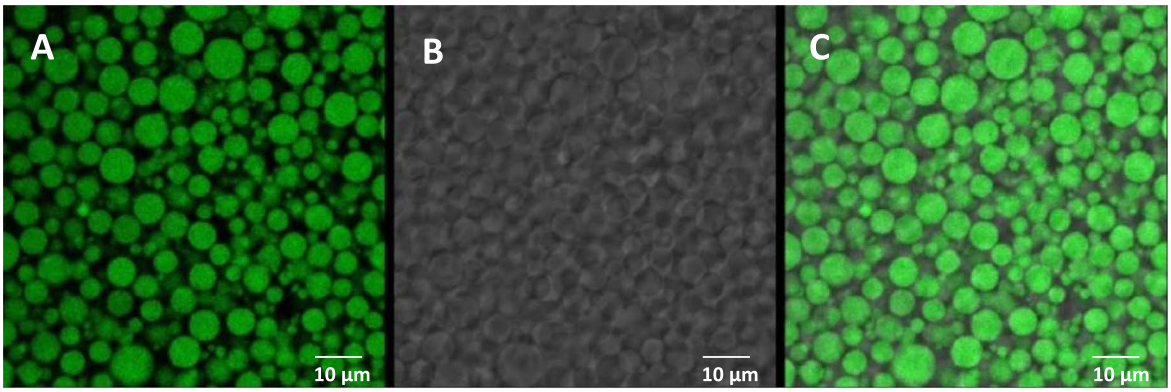

Fig. 1. Confocal snapshots of AF 488 labeled RNase A (green) in dispersion of anionic dex-MA-co-MA microgels (DS 8, 60% water content, 800 µl MA), (A) AF 488 RNase A loaded microgels, (B) Bright field, (C) merged. Scale bar 10 µm. (For interpretation of the references to colour in this figure legend, the reader is referred to the web version of this article.)

2.11. PEI coating of RNase A loaded nanogels

To coat nanogels with polyethyleneimine (PEI), 2 mg of empty and RNase A loaded nanogels were dispersed in 0.5 ml HEPES buffer (20 mM, pH 7.4). A solution of 0.5 mg of PEI in 0.5 ml HEPES buffer (20 mM, pH 7.4) was added to the particle dispersion. The mixture was subsequently sonicated (Tip sonicator, amplitude 10%) for 20 s and the PEI-coated particles were washed 2 times with PBS and recovered by centrifugation. The ζ-potential of coated particles dispersed in 10 mM HEPES buffer pH 7.4 was measured by Zetasizer Nano-Z (Malvern Instrument Ltd.). The average size and size distribution were determined by dynamic light scattering (DLS, Malvern ALV/CGS-3 Goniometer, Malvern, UK) at 25 °C.

2.12. Release of RNase A from nanogels

Dried RNase A loaded nanogels with and without PEI coating (prepared as described in Sections 2.10. and 2.11. respectively) were dispersed in PBS at a concentration of 5 mg/ml. The homogeneous nanogel suspension was aliquoted into eppendorf tubes that were subsequently incubated at 37 °C under mild agitation. For triggered release of conjugated RNase A, a solution of glutathione PBS was added after 8 h at a concentration of 2.5 mM and after 14 h to a final concentration of 10 mM. At different time points, a sample was centrifuged (15,000 rpm, 1 h) and the supernatant was collected and the amount of released RNase A was measured by UPLC (Acquity UPLC®, Waters Corporation, Milford, USA) equipped with a BEH300 C18 1.7 µm column. Solvent mixtures consisting of 5% ACN/95% H_2O/0.1% (TFA) and 100% ACN/0.1% TFA were used as eluent A and B, respectively. A gradient was run from 0 to 60% B in 7 min with a flow rate of 0.25 ml/min. The injection volume was 7.5 µl and the detection wavelength was 280 nm. The calibration curve was linear between 50 and 1000 µg/ml. In addition, the release of RNase A from nanogels with physically loaded protein was measured as a control.

2.13. Cell culture

The human breast cancer cell line MDA-MB-231 (ATCC® CRM-HTB-26™) was obtained from American Type Culture Collection (ATCC, LGC Standards GmbH, Wesel, Germany) and cultured in Dulbecco's Modified Eagle's Medium (DMEM, Gibco) with 10% (v/v) FBS at 37 °C in a humidified atmosphere containing 5% CO_2.

2.13.1. Cellular uptake of nanogels (Confocal laser scanning microscopy)

MDA-MB 231 cells were seeded into a 96 well-plate at a density of 10^4 cells/well. After 24 h, 100 µl of Alexa Fluor 647 labeled nanogels (12.5 µg/ml) without and with AF 488 labeled PEI coating were added to the cells and incubated for 4 h (37 °C, 5% CO_2). Subsequently, the cells were washed with phosphate-buffered saline (Dulbecco's Phosphate Buffered Saline, 0.2 g/L KCl, 0.2 g/L KH_2PO_4, 8.0 NaCl, 1.15 g/L Na_2HPO_4) and fresh culture medium was added. The intracellular fluorescence distribution was visualized using a Yokogawa CV7000s high-content imager (Yokogawa, Tokyo, Japan) at 60× magnification. Live-cell images in three channels were captured, Hoechst 33342 (excitation 350 nm, emission 461 nm) to visualize nuclei, Alexa Fluor® 647 (excitation 649 nm, emission 666 nm) to observe nanogels and Alexa Fluor® 488 (excitation 498 nm, emission 520 nm) to detect PEI coated nanogels.

2.13.2. Cytotoxicity assay of RNase A loaded nanogels

The cytotoxicity of RNase A loaded nanogels with and without PEI coating was determined by cell viability assay. In brief, MDA-MB-231 cells were seeded in a 96-well plate at the density of 10,000 cells/100 µl growth medium (DMEM, supplemented with 10% FBS) per well and cultured in a humidity controlled incubator (5% CO_2 at 37 °C) 24 h before the MTS assay was performed. Subsequently, the medium was replaced with 100 µl fresh medium containing 1% antibiotics. Nanogel (different compositions) suspensions (100 µl) in culture medium at concentrations of 0.25, 0.5, 0.75, and 1 mg/ml were incubated with the cells. Cell viability was evaluated after 24 h using a colorimetric MTS cell proliferation kit, according to the manufacturer's instructions. Cells incubated with solutions of RNase A and Traut's modified RNase A (concentrations ranging from 3.125 to 25 µM) were taken as controls.

2.13.3. Apoptosis assay of RNase A loaded nanogels (Caspase activity Assay)

To investigate the caspase-mediated apoptotic pathway, commercially available CellEvent™ caspase-3/7 Green Detection Reagent was used. Cells were seeded at a density of 10,000 cells/well into a 96 well-plate and allowed to adhere overnight. The cells were treated with 100 µl of empty and RNase A loaded nanogels with PEI coating (0.25–1 mg/ml) dispersed in culture medium and the diluted CellEvent™ Caspase-3/7 Green Detection Reagent at a final concentration of 10 µM in complete medium was added to each well and incubated for 30 min. Confocal imaging was performed on an automated Yokogawa CV7000s spinning disk microscope. The images were taken every 2 h for 24 h. The fluorescence intensity of apoptotic cells was then quantified with Columbus Software (U.S. National Institutes of Health, Bethesda, Maryland, USA).

3. Results and discussion

3.1. Preparation and characterization of anionic dextran nanogels

Anionic and neutral dextran-based nanogels were obtained by free radical copolymerization of Dex-MA with sodium methacrylate and 2-

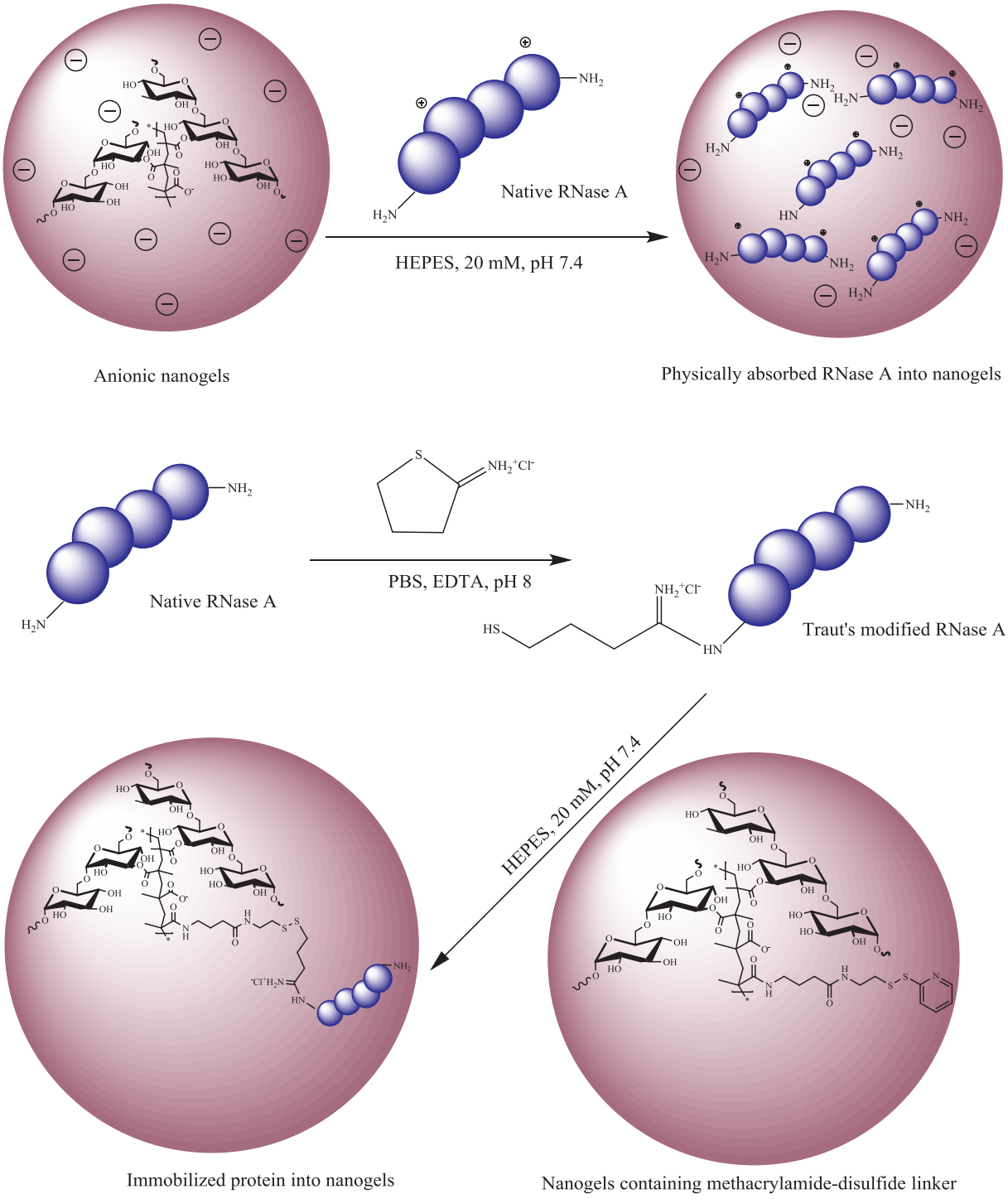

Scheme 1. Reaction scheme for protein absorption into anionic nanogels, Traut's modification of RNase A and disulfide bonds formation with linker presented in nanogels.

hydroxyethyl methacrylate, respectively. The characteristics of the different formulations are reported in Table 1. As indicated, all formulations were obtained in good yields (74–92%). The hydrodynamic diameter of the different nanogels was between 200 and 250 nm with an acceptable polydispersity index (0.08–0.27). The nanogels prepared from dex-MA and HEMA had a slightly negative charge (−1.9 mV), which is in line with previous reports [35]. By adding sodium methacrylate (SMA), the zeta potential of the obtained nanogels decreased with increasing amount of SMA in the formulation (−1.9 to −32.5 mV; Table 1), which demonstrates that sodium methacrylate was indeed incorporated in the hydrogel network.

In parallel, microgels were prepared using a water-in-water emulsion method, and anionic dex-MA-co-MA microgels with different water content (and thus different crosslink density) and zeta potential were obtained (Table 2). The microgels were used to enable visualization of the protein absorption process since this was not possible with the nanogels, because it is difficult to distinguish between adsorbed and absorbed protein. Similar to the nanogels, the microgels showed a tunable negative surface charge depending on the concentration methacrylic acid used as revealed from zeta potential measurements. In our further experiments, dex-MA-co-MA microgels (DS 8, 60% water content, 800 µl MA) were used to visualize the distribution of the

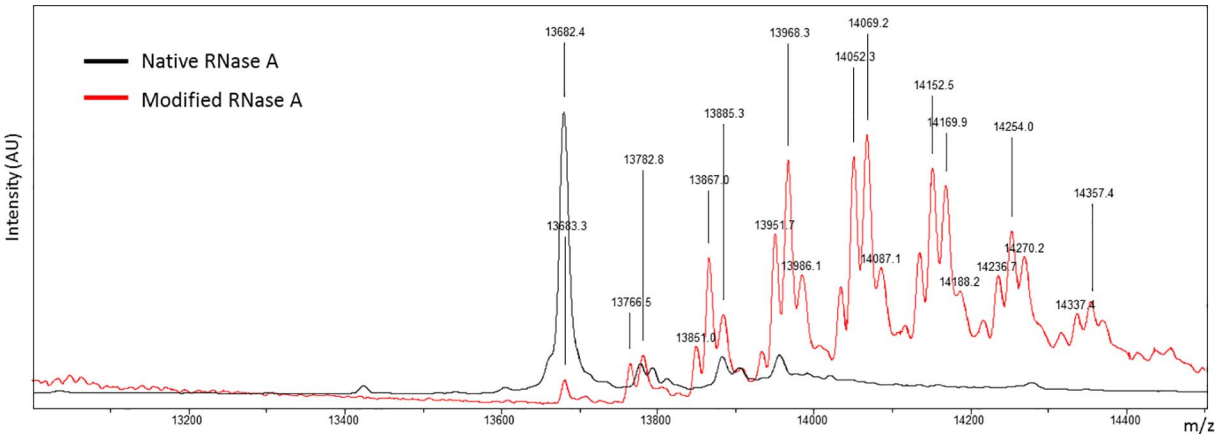

Fig. 2. Deconvoluted ESI-TOF MS spectrum of 2-iminothiolane modified RNase A, Traut's: RNase A (10:1 mol:mol).

Table 3
Characterization of RNase A loaded dex-MA-co-MA nanogels. Mean values with corresponding standard deviations are shown (n = 3).

Linker containing dex-MA-co-MA nanogels	Z_{ave} (nm)	ζ-potential (mV)	Loading efficiency[a] (%)	Loading content[b] (%)
Empty nanogels	205 ± 5	−21.7 ± 0.8	NA	NA
RNAse A loaded nanogels	212 ± 6	−18.0 ± 0.9	75 ± 3	20.1 ± 0.9
PEI coated RNase A nanogels[c]	215 ± 3	+8.1 ± 0.3	72 ± 6	19.3 ± 1.1

[a] Loaded RNase A in nanogels/feed RNase A weight × 100%.
[b] Loaded RNase A/RNase A loaded nanogels weight × 100%.
[c] Nanogels: PEI 1:0.2 (wt:wt).

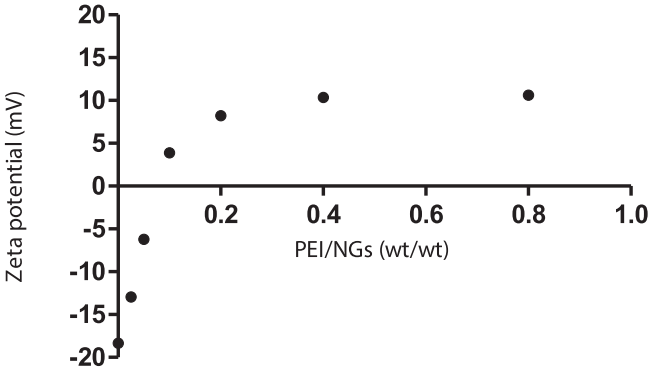

Fig. 3. ζ-potential of RNase A loaded nanogels after polyethyleneimine coating, measured in HEPES buffer 10 mM, pH 7.4, n = 3, The SD's are smaller than the symbols.

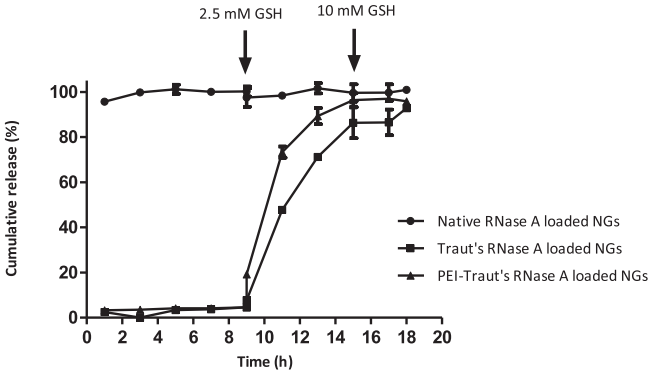

Fig. 4. Release of RNase A from dex-MA nanogels in PBS pH 7.4 at 37 °C; glutathione was added to 2.5 mM final concentration at 7 h and to 10 mM at 15 h, n = 3.

absorbed labeled protein (Alexa Fluor™ 488). The confocal image illustrates that RNase A was indeed able to diffuse into and distributed homogeneously in anionic nanogels within 1 h (Fig. 1A–C). This rapid absorption can be explained by the electrostatic interaction between the negative charge of microgels and net positive charge of RNase A at neutral pH (pI 9.3) [59]. This result is in accordance with previous studies which have also shown diffusion of a positively charged protein, lysozyme (pI 11.35), into dextran-based negatively charged microspheres, whereas this protein was unable to absorb into positively charged microspheres [60].

A disulfide-containing linker, *N*-(4-(2-(pyridine-2-yldisulfanyl) ethyl)-amidobutyl) methacrylamide, was synthesized and copolymerized with dex-MA and SMA to yield nanogels. This linker was used to covalently immobilize the protein in the nanogels via disulfide bonds aiming at the triggered release of the protein under reducing conditions. The incorporation efficiency of the pyridyl disulfide linker in nanogels was quantified by measuring of the 2-mercaptopyridine released from nanogels after incubation with DTT. HPLC analysis showed that 20 ± 2% of linker present in the feed was incorporated in the nanogels network which is in agreement with our previous study [35].

3.2. Modification of RNase A with 2-iminothiolane

To covalently conjugate RNase A to linker containing nanogels, we functionalized the protein with thiol groups using 2-iminothiolane (Traut's reagent). This reagent reacts with primary amines of RNase A without altering the overall positive charge of the protein [61], which is necessary for the absorption process (Scheme 1). RNase A has 10 amine groups in the form of lysine units [62]. The results of Ellman's assay show that on the average three thiol (–SH) groups were introduced to the RNase A by using a feed molar ratio of 10:1 (2-iminothiolane: protein). Furthermore, by using a 50–100 M excess of 2-iminothilane, ~7 thiol groups were introduced in the protein (Fig. S2), indicating that 7 lysine residues are accessible for the reaction with 2-iminothiolane. The UPLC chromatogram of modified RNase (10:1, Traut:RNase A) showed a single peak with the same retention time as native RNase, indicating that the primary structure of the modified protein was retained and that the modified protein has the same affinity for the stationary phase as native RNase (Fig. 1S) which might be ascribed to the fact that the overall charge of the protein has not changed after introduction of thiols groups. The mass spectrum of modified RNase A shows the distribution of masses corresponding to different numbers of modifications with 2-iminothiolane. The difference between the peaks is 101 Da, which corresponds to the mass of one 2-iminothiolane molecule. Native RNase A has a molecular weight of 13683 Da and after modification of primary amine groups, multiple peaks were detected in the mass spectrum indicating a mixture of species with 2–7 2-

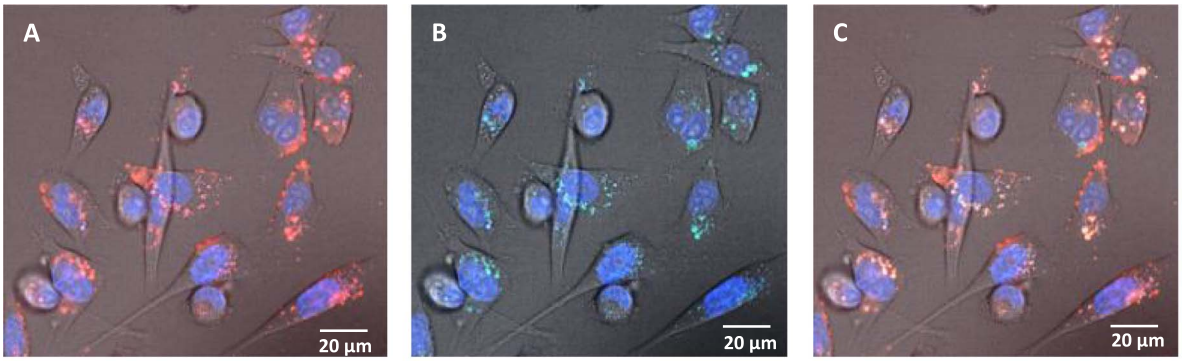

Fig. 5. Confocal images of the intracellular distribution of PEI coated dex-MA nanogels in MDA-MB 231 cells. (A) Alexa Fluor 647 labeled nanogels (red), (B) Alexa Fluor 488 labeled PEI coating (green), (C) overlay image of green and red fluorescence. PEI coated nanogels (12.5 µg mL^{-1}) were incubated for 4 h at 37° C. Nuclei were labeled with Hoechst 33342 (blue). (For interpretation of the references to colour in this figure legend, the reader is referred to the web version of this article.)

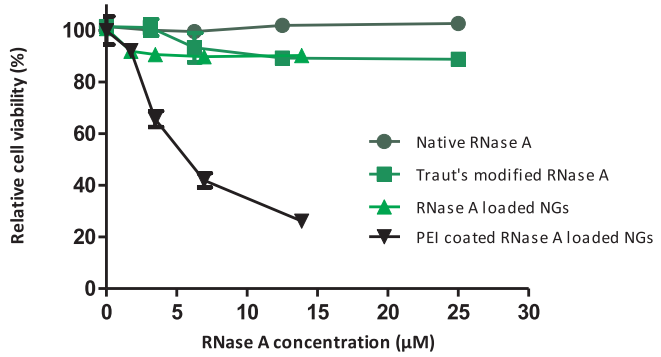

Fig. 6. Cell viability of MDA-MB 231 cells upon 24 h incubation with native RNase A, modified RNase A, RNase A-loaded NGs and PEI coated RNase A loaded nanogels, n = 3.

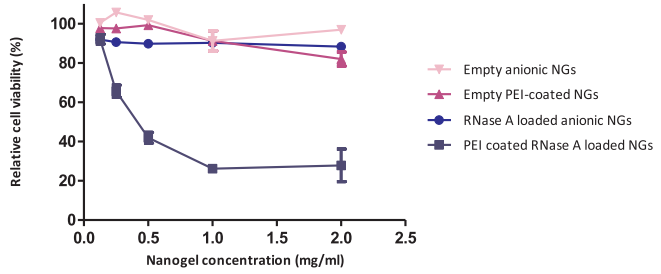

Fig. 7. Cell viability of MDA-MB 231 cells upon 24 h incubation with empty anionic nanogels, empty PEI coated nanogels, RNase A-loaded NGs and PEI coated RNase A loaded nanogels, n = 3.

iminothiolane groups per RNase A (Fig. 2). This result is in line with the Ellman's assay of modified RNase A (Fig. 2S).

The enzymatic activity of Traut's modified RNase A (10:1, Traut:RNase A) was assessed by digestion of yeast RNA. This assay showed that 86% of the biological activity of RNase A was retained after modification with Traut's reagent.

3.3. Post loading and covalent conjugation of modified RNase A

RNase A was loaded into the nanogels network (250 µmol SMA) via a charge driven process in a buffer of low ionic strength. Since the protein is released from nanogels at physiological conditions (pH 7.4, 150 mM NaCl), the electrostatically driven post loaded RNase A was covalently immobilized into the gel network via reducible disulfide bonds. To this end, the introduced thiol groups of RNase A were coupled to the network via a disulfide exchange reaction of free thiols of the protein and disulfide bonds of the linker present in dex-MA-co-MA nanogels (Scheme 1).

Empty anionic nanogels were prepared by photo-copolymerization of Dex-MA sodium methacrylate and the linker containing pyridyldisulfide. The obtained empty nanogels had a zeta potential (−21.7 mV) and hydrodynamic diameter around 200 nm with a relatively low PDI (< 0.3). After covalent immobilization of modified RNase A into these nanogels, the zeta potential of particles slightly changed (−18.0 mV), which can be ascribed to neutralization of the negative charge of the nanogels by the positively charged RNase A. High loading content (≈20%) and loading efficiency (≈75%) of protein in the particles was achieved in both non-coated and PEI coated nanogels (Table 3).

3.4. PEI coating of RNase A loaded nanogels

Cellular uptake study using confocal microscopy showed that non-coated anionic nanogels were hardly internalized by MDA-MB 231 cell line (Fig. 4S and Section 3.6), which is in agreement with previous findings [63].

Hence, to reverse the zeta potential, the anionic nanogels were coated with polyethyleneimine. It has been shown that this cationic polymer is able to bind to the cell membranes and particles coated with this polymer are internalized through endocytosis in general [64,65]. Fig. 3 shows that the zeta potential increased from −18.3 mV for non-coated nanogels to −12.9 mV for a formulation with a nanogels:PEI weight ratio of 1:0.025. By increasing the amount of PEI in the feed to 1:0.8 nanogels:PEI weight ratio, the zeta-potential of the particles increased to +10.6 mV. The size of the nanogels did not change substantially after PEI modification (212 nm for non-coated and 225 nm for coated with a ratio of 1:0.8), indicating that PEI did not induce nanogel aggregation. Considering the zeta potential of coated nanogels, the 1:0.2 (wt/wt) ratio of particle:polymer was chosen for subsequent cellular uptake and cytotoxicity experiments. The coated particles with this ratio carry a sufficient zeta potential (+8.1 mV) enabling cellular uptake. On the other hand, it has been shown that particles with a high zeta potential can aggregate due to interaction with proteins present in cell culture media e.g. the circulation and the extracellular environment [66] excluding them for further evaluations.

3.5. In vitro release of RNase A from nanogels

Fig. 4 shows that the physically bound native RNase A was fully desorbed/released from anionic nanogels by dispersion of the nanoparticles in physiological buffer (PBS) at the first measuring time point (1h), whereas Traut's modified RNase A was stably encapsulated indicating covalent conjugation of this modified protein to the hydrogel network through a thiol-disulfide exchange reaction. Interestingly, more than 90% of the immobilized protein was released after incubating with PBS buffer containing 10 mM glutathione which

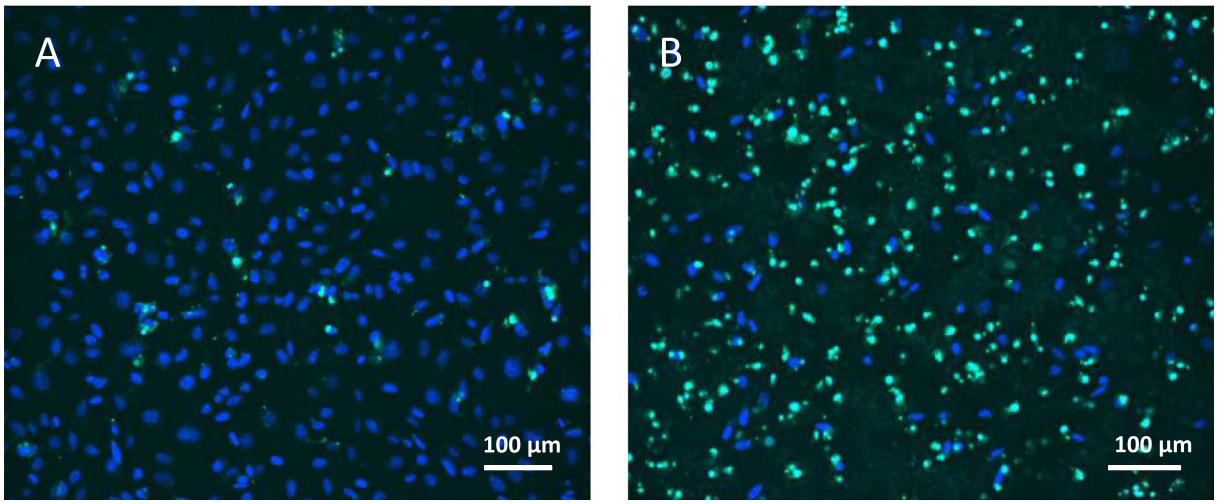

Fig. 8. Confocal microscopy images of activation of caspase-3/7 in apoptotic MDA-MB 231 cells after 24 h incubation with (A) Empty PEI coated nanogels, (B) RNase A loaded PEI coated nanogels. Cell nuclei were stained with Hoechst 33,342 (blue). (For interpretation of the references to colour in this figure legend, the reader is referred to the web version of this article.)

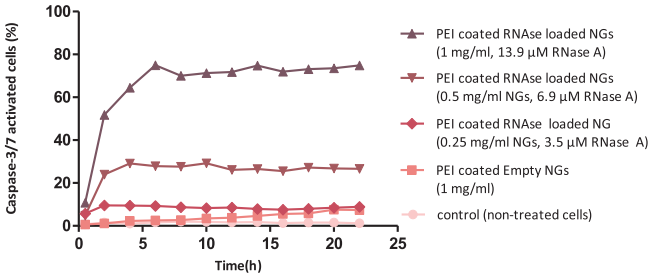

Fig. 9. RNase A-induced apoptosis by activation of caspase-3/7 in MDA-MB cells.

corresponds with intracellular levels [37]. These observations are in line with our previous study showing the reduction-sensitivity of disulfide bridges in ovalbumin-loaded nanogels [35]. Importantly, a similar trend was observed for PEI coated nanogels which demonstrates that the polymer coating has no significant influence on the triggered release of RNase.

3.6. Cellular uptake study of nanogels

The cellular uptake of the different nanogel formulations by MDA-MB 231 cells was monitored using confocal microscopy. To visualize the cellular internalization, the dex-MA-co-MA nanogels were labeled with Alexa Fluor® 647 (non-coated formulation) and labeled nanogels were coated with Alexa Fluor® 488 labeled PEI (coated formulation). Confocal images of MDA-MB 231 cells showed that the non-coated nanogels were barely taken up by the cells (Fig. 4S), whereas PEI coated nanogels were efficiently internalized by the cells after 4 h, revealing the crucial role of surface charge of particles in cellular uptake in line with previous studies [63]. In addition, the fluorescent signal of the polymer coating was observed inside cells overlapping with the signal of Alexa Fluor® 647-nanogels (Fig. 5C) indicating colocalization of PEI and nanogels in cellular compartments.

3.7. Cytotoxic activity of RNase A loaded nanogels

The cytotoxic effect of PEI coated RNase-loaded NGs, RNase-loaded NGs, native and Traut's modified RNase A in their soluble forms was examined in MDA-MB 231 cell line using the MTS assay. As shown in Fig. 6, both native and modified RNase A did not show cytotoxic activity most likely due to its insufficient cellular uptake [50]. Furthermore, the non-coated nanogels did not affect cell viability significantly even at the highest concentration of RNase A, indicating that anionic nanoparticles have poor interaction with negatively charged cell surface resulting in poor uptake (Section 3.6) which is in agreement with previous reports [63]. The PEI-coated nanogels without RNase loading showed some cytotoxicity at the highest dose tested (2 mg/ml) (Fig. 7) which might be ascribed to the cytotoxic effect of PEI [67,68]. Importantly, the PEI coated nanogels loaded with RNase A exhibited a concentration-dependent cytotoxic effect after 24 h incubation with cancer cells. This can be explained by the positive surface charge of this particle leading to high cellular uptake (Fig. 6) [67,69] and subsequent intracellular release of RNase A. The release of RNase occurs either in the endosome followed by endosomal escape due to action of PEI or after endosomal escape of the nanogels and release of the enzyme in the cytosol. It has been reported that PEI is able to destabilize lysosomal membranes through the so-called "proton sponge effect", which promotes the endosomal escape of particles and their release into the cytoplasm [70–73].

3.8. Caspase activity assay

PEI coated RNase A loaded nanogels were assessed for their capability to induce apoptosis using CellEvent™ Caspase-3/7 Green Detection Reagent. The probe consists of a quenching peptide conjugated to a nucleic acid–binding dye which does not give fluorescence in healthy cells. Upon activation, caspases 3/7 cleave the inhibiting peptide from the dye, which subsequently binds to cell DNA and results in bright green fluorescence (absorption/emission maxima of ~502/530 nm) [74,75]. Confocal images of MDA-MB 231 cells treated with PEI coated empty nanogels and PEI coated RNase A nanogels are depicted in Fig. 8. Incubation of cells with PEI-coated nanogels without RNase loading as a control showed a limited fluorescent signal of apoptotic cells after 24 h, whereas a strong signal was observed when the cells were incubated with PEI-coated RNase A loaded nanogels demonstrating that RNase A-induced apoptosis occurred. Fig. 9 shows the apoptosis activation kinetics of cells incubated with PEI coated empty NGs (different concentrations) for 22 h. The percentage of caspase-activated cells incubated with empty PEI coated nanogels at the highest concentration of nanogels (1 mg/ml) was < 10%, while caspase activation was evident in cells incubated with RNase A loaded nanogels at different concentrations. It should be noted that the used probe allows the detection of early caspase-3/7 activation after which cells irreversibly undergo apoptosis. These results are in line with previous findings of Magun et al. who demonstrated that caspase-3/7 activation was observed as early as 1–2 h after Onconase incubation while the release of cytochrome C (a marker for cell death) was delayed [76,77].

Importantly, the percentage of apoptotic cells induced by RNase A loaded NGs was dose-dependent, which is in good agreement with cell viability study reported in Section 3.7. These findings illustrate that by catalyzing the degradation of cytosolic RNAs, intracellular released RNase A inhibits the protein synthesis and induces apoptotic cell death [78].

4. Conclusions

In this study, we designed dex-MA nanogels loaded with RNase A as a nanocarrier for cancer therapy. The immobilized RNase A was hardly released from the nanogels under non-reductive conditions while the protein was completely released under reductive conditions. A high intracellular delivery efficiency of dex-MA- nanogels was obtained by coating the negatively charged surface of nanogels with a cationic polymer (polyethyleneimine). It is further shown that PEI coated RNase A loaded nanogels induced cell death via apoptosis. It can therefore be concluded that PEI coated nanogels are highly interesting delivery vehicles to exploit the therapeutic potential of RNase A for cancer treatment.

Acknowledgments

The research was support from the Innovative Medicines Initiative Joint Undertaking under grant agreement no. 115363 (IMI-COMPACT), resources of which are composed of financial contribution from the European Union's Seventh Framework Programme (FP7/2007- 2013) and EFPIA companies in kind contribution.

Appendix A. Supplementary data

Supplementary data associated with this article can be found, in the online version, at http://dx.doi.org/10.1016/j.cej.2017.12.071.

References

[1] B. Leader, Q.J. Baca, D.E. Golan, Protein therapeutics: a summary and pharmacological classification, Nat. Rev. Drug Discov. 7 (2008) 21–39.
[2] P.J. Carter, Introduction to current and future protein therapeutics: a protein engineering perspective, Exp. Cell Res. 317 (2011) 1261–1269.
[3] B. Meibohm, Pharmacokinetics and pharmacodynamics of peptide and protein therapeutics, in: D.J.A. Crommelin, R.D. Sindelar, B. Meibohm (Eds.), Pharmaceutical Biotechnology: Fundamentals and Applications, forth ed., Springer, New York, 2013, pp. 101–132.
[4] V. Torchilin, Intracellular delivery of protein and peptide therapeutics, Drug Discov. Today 5 (2008) 95–103.
[5] A. Fu, R. Tang, J. Hardie, M.E. Farkas, V.M. Rotello, Promises and pitfalls of intracellular delivery of proteins, Bioconjug. Chem. 25 (2014) 1602–1608.
[6] S. Mitragotri, P.A. Burke, R. Langer, Overcoming the challenges in administering biopharmaceuticals: formulation and delivery strategies, Nat. Rev. Drug Discov. 13 (2014) 655–672.
[7] S. Frokjaer, D.E. Otzen, Protein drug stability: a formulation challenge, Nat. Rev. Drug Discov. 4 (2005) 298–306.
[8] P.L. Campbell, J. McCluskey, J.P. Yeo, B.-H. Toh, Electroporation of antibodies into mammalian cells, in: J.A. Nickoloff (Ed.), Animal Cell Electroporation and Electrofusion Protocols, Humana Press, Totowa, NJ, 1995, pp. 83–92.
[9] K. Nolkrantz, C. Farre, K.J. Hurtig, P. Rylander, O. Orwar, Functional screening of intracellular proteins in single cells and in patterned cell arrays using electroporation, Anal. Chem. (2002) 4300–4305.
[10] Y. Zhang, L.C. Yu, Single-cell microinjection technology in cell biology BioEssays news and reviews in molecular, Cell. Dev. Biol. (2008) 606–610.
[11] W.J. Buchser, J.R. Pardinas, Y. Shi, J.L. Bixby, V.P. Lemmon, 96-Well electroporation method for transfection of mammalian central neurons, Biotechniques 41 (2006) 619–624.
[12] S.B. Fonseca, M.P. Pereira, S.O. Kelley, Recent advances in the use of cell-penetrating peptides for medical and biological applications, Adv. Drug Deliv. Rev. 61 (2009) 953–964.
[13] S. Deshayes, M.C. Morris, G. Divita, F. Heitz, Cell-penetrating peptides: tools for intracellular delivery of therapeutics, Cell. Mol. Life Sci. 62 (2005) 1839–1849.
[14] F. Wang, Y. Wang, X. Zhang, W. Zhang, S. Guo, F. Jin, Recent progress of cell-penetrating peptides as new carriers for intracellular cargo delivery, J. Control. Release 174 (2014) 126–136.
[15] A.T. Jones, E.J. Sayers, Cell entry of cell penetrating peptides: tales of tails wagging dogs, J. Control. Release 161 (2012) 582–591.
[16] S. Reissmann, Cell penetration: scope and limitations by the application of cell-penetrating peptides, J. Pept. Sci. 20 (2014) 760–784.
[17] R. Tang, C.S. Kim, D.J. Solfiell, S. Rana, R. Mout, E.M. Velázquez-Delgado, A. Chompoosor, Y. Jeong, B. Yan, Z.-J. Zhu, C. Kim, J.A. Hardy, V.M. Rotello, Direct delivery of functional proteins and enzymes to the cytosol using nanoparticle-stabilized nanocapsules, ACS Nano 7 (2013) 6667–6673.
[18] M.E. El-Sayed, A.S. Hoffman, P.S. Stayton, Smart polymeric carriers for enhanced intracellular delivery of therapeutic macromolecules, Expert. Opin. Biol. Ther. 5 (2005) 23–32.
[19] O. Zelphati, Y. Wang, S. Kitada, J.C. Reed, P.L. Felgner, J. Corbeil, Intracellular delivery of proteins with a new lipid-mediated delivery system, J. Biol. Chem. 276 (2001) 35103–35110.
[20] Y. Lee, T. Ishii, H. Cabral, H.J. Kim, J.H. Seo, N. Nishiyama, H. Oshima, K. Osada, K. Kataoka, Charge-conversional polyionic complex micelles-efficient nanocarriers for protein delivery into cytoplasm, Angew. Chem. 48 (2009) 5309–5312.
[21] B. Yameen, W.I. Choi, C. Vilos, A. Swami, J. Shi, O.C. Farokhzad, Insight into nanoparticle cellular uptake and intracellular targeting, J. Control Release 190 (2014) 485–499.
[22] E. Blanco, H. Shen, M. Ferrari, Principles of nanoparticle design for overcoming biological barriers to drug delivery, Nat. Biotechnol. 33 (2015) 941–951.
[23] Y. Jiang, J. Chen, C. Deng, E.J. Suuronen, Z. Zhong, Click hydrogels, microgels and nanogels: emerging platforms for drug delivery and tissue engineering, Biomaterials 35 (2014) 4969–4985.
[24] K. Raemdonck, B. Naeye, K. Buyens, R.E. Vandenbroucke, A. Høgset, J. Demeester, S.C. De Smedt, Biodegradable dextran nanogels for RNA interference: focusing on endosomal escape and intracellular siRNA delivery, Adv. Funct. Mater. 19 (2009) 1406–1415.
[25] H. Zhang, Y. Zhai, J. Wang, G. Zhai, New progress and prospects: the application of nanogel in drug delivery, Mater. Sci. Eng. C Mater. Biol. Appl. 60 (2016) 560–568.
[26] D. Li, C.F. van Nostrum, E. Mastrobattista, T. Vermonden, W.E. Hennink, Nanogels for intracellular delivery of biotherapeutics, J. Control Release 259 (2017) 16–28.
[27] K.S. Soni, S.S. Desale, T.K. Bronich, Nanogels: an overview of properties, biomedical applications and obstacles to clinical translation, J. Control. Release 240 (2016) 109–126.
[28] E.S. Dragan, Design and applications of interpenetrating polymer network hydrogels. A review, 2014.
[29] S.J. Buwalda, K.W. Boere, P.J. Dijkstra, J. Feijen, T. Vermonden, W.E. Hennink, Hydrogels in a historical perspective: from simple networks to smart materials, J. Control Release 190 (2014) 254–273.
[30] M. Hamidi, A. Azadi, P. Rafiei, Hydrogel nanoparticles in drug delivery, Adv. Drug. Delivery Rev. 60 (2008) 1638–1649.
[31] W.E. Hennink, C.F. van Nostrum, Novel crosslinking methods to design hydrogels, Adv. Drug. Delivery Rev. 54 (2002) 13–36.
[32] T. Vermonden, R. Censi, W.E. Hennink, Hydrogels for protein delivery, Chem. Rev. 112 (2012) 2853–2888.
[33] N.A. Peppas, J.Z. Hilt, A. Khademhosseini, R. Langer, Hydrogels in biology and medicine: from molecular principles to bionanotechnology, Adv. Mater. 18 (2006) 1345–1360.
[34] Y. Li, D. Maciel, J. Rodrigues, X. Shi, H. Tomás, Biodegradable polymer nanogels for drug/nucleic acid delivery, Chem. Rev. 115 (2015) 8564–8608.
[35] D. Li, N. Kordalivand, M.F. Fransen, F. Ossendorp, K. Raemdonck, T. Vermonden, W.E. Hennink, C.F. van Nostrum, Reduction-sensitive dextran nanogels aimed for intracellular delivery of antigens, Adv. Funct. Mater. 25 (2015) 2993–3003.
[36] M.R. Molla, T. Marcinko, P. Prasad, D. Deming, S.C. Garman, S. Thayumanavan, Unlocking a caged lysosomal protein from a polymeric nanogel with a pH trigger, Biomacromolecules 15 (2014) 4046–4053.
[37] F. Meng, W.E. Hennink, Z. Zhong, Reduction-sensitive polymers and bioconjugates for biomedical applications, Biomaterials 30 (2009) 2180–2198.
[38] L. Brülisauer, M.A. Gauthier, J.-C. Leroux, Disulfide-containing parenteral delivery systems and their redox-biological fate, J. Control Release 195 (2014) 147–154.
[39] R. Cheng, F. Feng, F. Meng, C. Deng, J. Feijen, Z. Zhong, Glutathione-responsive nano-vehicles as a promising platform for targeted intracellular drug and gene delivery, J. Control Release 152 (2011) 2–12.
[40] C. Yu, C. Gao, S. Lü, C. Chen, Y. Huang, M. Liu, Redox-responsive shell-sheddable micelles self-assembled from amphiphilic chondroitin sulfate-cholesterol conjugates for triggered intracellular drug release, Chem. Eng. J. 228 (2013) 290–299.
[41] M.S. Hillwig, A.L. Contento, A. Meyer, D. Ebany, D.C. Bassham, G.C. MacIntosh, RNS2, a conserved member of the RNase T2 family, is necessary for ribosomal RNA decay in plants, Proc. Natl. Acad. Sci. U.S.A. 108 (2011) 1093–1098.
[42] K. Baumgardt, H. Melior, R. Madhugiri, S. Thalmann, A. Schikora, M. McIntosh, A. Becker, E., Evguenieva-Hackenberg, RNase E and RNase J are needed for S-adenosylmethionine homeostasis in Sinorhizobium meliloti, Microbiol. (Reading, England) 163 (2017) 570–583.
[43] W. Ardelt, B. Ardelt, Z. Darzynkiewicz, Ribonucleases as potential modalities in anticancer therapy, Eur. J. Pharmacol. 625 (2009) 181–189.
[44] I. Lee, A. Kalota, A.M. Gewirtz, K. Shogen, Antitumor efficacy of the cytotoxic RNase, ranpirnase, on A549 human lung cancer xenografts of nude mice, Anticancer Res. 27 (2007) 299–307.
[45] R.J. Youle, D. Newton, Y.N. Wu, M. Gadina, S.M. Rybak, Cytotoxic ribonucleases and chimeras in cancer therapy, Crit. Rev. Ther. Drug Carrier Syst. 10 (1993) 1–28.
[46] P.A. Leland, R.T. Raines, Cancer chemotherapy — Ribonucleases to the rescue, Chem. Biol. 8 (2001) 405–413.
[47] J.W. Baynes, F. Wold, Effect of glycosylation on the in vivo circulating half-life of ribonuclease, J. Biol. Chem. 251 (1976) 6016–6024.
[48] S.K. Saxena, S.M. Rybak, G. Winkler, H.M. Meade, P. McGray, R.J. Youle, E.J. Ackerman, Comparison of RNases and toxins upon injection into Xenopus oocytes, J. Biol. Chem. 266 (1991) 21208–21214.

[49] D.L. Newton, O. Ilercil, D.W. Laske, E. Oldfield, S.M. Rybak, R.J. Youle, Cytotoxic ribonuclease chimeras. Targeted tumoricidal activity in vitro and in vivo, J. Biol. Chem. 267 (1992) 19572–19578.
[50] J.H. Choi, J.Y. Jang, Y.K. Joung, M.H. Kwon, K.D. Park, Intracellular delivery and anti-cancer effect of self-assembled heparin-Pluronic nanogels with RNase A, J. Control. Release 147 (2010) 420–427.
[51] X. Liu, P. Zhang, W. Rödl, K. Maier, U. Lächelt, E. Wagner, Toward artificial immunotoxins: traceless reversible conjugation of RNase A with receptor targeting and endosomal escape domains, Mol. Pharm. 14 (2017) 1439–1449.
[52] X. Wang, Y. Li, Q. Li, C.I. Neufeld, D. Pouli, S. Sun, L. Yang, P. Deng, M. Wang, I. Georgakoudi, S. Tang, Q. Xu, Hyaluronic acid modification of RNase A and its intracellular delivery using lipid-like nanoparticles, J. Control. Release 263 (2017) 39–45.
[53] W.N.E. van Dijk-Wolthuis, O. Franssen, H. Talsma, M.J. van Steenbergen, J.J. Kettenes-van den Bosch, W.E. Hennink, Synthesis, characterization, and polymerization of glycidyl methacrylate derivatized dextran, Macromolecules 28 (1995) 6317–6322.
[54] W.N.E. van Dijk-Wolthuis, J.J. Kettenes-van den Bosch, A. van der Kerk-van Hoof, W.E. Hennink, Reaction of dextran with glycidyl methacrylate: an unexpected transesterification, Macromolecules 30 (1997) 3411–3413.
[55] R.J.H. Stenekes, O. Franssen, E.M.G. van Bommel, D.J.A. Crommelin, W.E. Hennink, The preparation of dextran microspheres in an all-aqueous system: effect of the formulation parameters on particle characteristics, Pharm. Res. 15 (1998) 557–561.
[56] J.M. Lambert, R. Jue, R.R. Traut, Disulfide crosslinking of Escherichia coli ribosomal proteins with 2-iminothiolane (methyl 4-mercaptobutyrimidate): evidence that the crosslinked protein pairs are formed in the intact ribosomal subunit, Biochemistry 17 (1978) 5406–5416.
[57] G.L. Ellman, Tissue sulfhydryl groups, Arch. Biochem. Biophys. 82 (1959) 70–77.
[58] G. Kalnitsky, H. Resnick, The effect of an altered secondary structure on ribonuclease activity, Chem. Biol. 234 (1959) 5.
[59] J.M. Messmore, R.T. Raines, Decavanadate inhibits catalysis by ribonuclease A, Arch. Biochem. Biophys. 381 (2000) 25–30.
[60] S.R. Van Tomme, B.G. De Geest, K. Braeckmans, S.C. De Smedt, F. Siepmann, J. Siepmann, C.F. van Nostrum, W.E. Hennink, Mobility of model proteins in hydrogels composed of oppositely charged dextran microspheres studied by protein release and fluorescence recovery after photobleaching, J. Control Release 110 (2005) 67–78.
[61] R. Singh, L. Kats, W.A. Blattler, J.M. Lambert, Formation of N-substituted 2-iminothiolanes when amino groups in proteins and peptides are modified by 2-iminothiolane, Anal. Biochem. 236 (1996) 114–125.
[62] R.T. Raines, Ribonuclease A, Chem. Rev. 98 (1998) 1045–1066.
[63] E. Fröhlich, The role of surface charge in cellular uptake and cytotoxicity of medical nanoparticles, Int. J. Nanomedicine 7 (2012) 5577–5591.
[64] K. Yu, J. Zhao, C. Yu, F. Sun, Y. Liu, Y. Zhang, R.J. Lee, L. Teng, Y. Li, Role of four different kinds of polyethylenimines (PEIs) in preparation of polymeric lipid nanoparticles and their anticancer activity study, J. Cancer 7 (2016) 872–882.
[65] J.M. Rosenholm, A. Meinander, E. Peuhu, R. Niemi, J.E. Eriksson, C. Sahlgren, M. Lindén, Targeting of porous hybrid silica nanoparticles to cancer cells, ACS Nano 3 (2009) 197–206.
[66] L. Nuhn, S. Gietzen, K. Mohr, K. Fischer, K. Toh, K. Miyata, Y. Matsumoto, K. Kataoka, M. Schmidt, R. Zentel, Aggregation behavior of cationic nanohydrogel particles in human blood serum, Biomacromolecules 15 (2014) 1526–1533.
[67] T. Xia, M. Kovochich, M. Liong, H. Meng, S. Kabehie, S. George, J.I. Zink, A.E. Nel, Polyethyleneimine coating enhances the cellular uptake of mesoporous silica nanoparticles and allows safe delivery of siRNA and DNA constructs, ACS Nano 3 (2009) 3273–3286.
[68] B.I. Florea, C. Meaney, H.E. Junginger, G. Borchard, Transfection efficiency and toxicity of polyethylenimine in differentiated Calu-3 and nondifferentiated COS-1 cell cultures, AAPS PharmSci 4 (2002) 1–11.
[69] K. Saha, S.T. Kim, B. Yan, O.R. Miranda, F.S. Alfonso, D. Shlosman, V.M. Rotello, Surface functionality of nanoparticles determines cellular uptake mechanisms in mammalian cells, Small 9 (2013) 300–305.
[70] H. Duan, S. Nie, Cell-penetrating quantum dots based on multivalent and endosome-disrupting surface coatings, J. Am. Chem. Soc. 129 (2007) 3333–3338.
[71] R.V. Benjaminsen, M.A. Mattebjerg, J.R. Henriksen, S.M. Moghimi, T.L. Andresen, The possible "Proton Sponge" effect of polyethylenimine (PEI) does not include change in lysosomal pH, Mol. Ther. 21 (2013) 149–157.
[72] M. Thomas, A.M. Klibanov, Enhancing polyethylenimine's delivery of plasmid DNA into mammalian cells, Proc. Natl. Acad. Sci. U.S.A. 99 (2002) 14640–14645.
[73] O. Boussif, F. Lezoualc'h, M.A. Zanta, M.D. Mergny, D. Scherman, B. Demeneix, J.P. Behr, A versatile vector for gene and oligonucleotide transfer into cells in culture and in vivo: polyethylenimine, Proc. Natl. Acad. Sci. U.S.A. 92 (1995) 7297–7301.
[74] S. Datz, C. Argyo, M. Gattner, V. Weiss, K. Brunner, J. Bretzler, C. von Schirnding, A.A. Torrano, F. Spada, M. Vrabel, H. Engelke, C. Brauchle, T. Carell, T. Bein, Genetically designed biomolecular capping system for mesoporous silica nanoparticles enables receptor-mediated cell uptake and controlled drug release, Nanoscale 8 (2016) 8101–8110.
[75] K.E. Burns, T.P. McCleerey, D. Thévenin, pH-selective cytotoxicity of pHLIP-antimicrobial peptide conjugates, Sci. Rep. 6 (2016) 1–10.
[76] T.-C. Huang, J.-F. Lee, J.-Y. Chen, Pardaxin, an antimicrobial peptide, triggers caspase-dependent and ROS-mediated apoptosis in HT-1080 cells, Mar. Drugs 9 (2011) 1995–2009.
[77] M.S. Iordanov, O.P. Ryabinina, J. Wong, T.H. Dinh, D.L. Newton, S.M. Rybak, B.E. Magun, Molecular determinants of apoptosis induced by the cytotoxic ribonuclease onconase: evidence for cytotoxic mechanisms different from inhibition of protein synthesis, Cancer Res. 60 (2000) 1983–1994.
[78] J. Castro, M. Ribo, S. Navarro, M.V. Nogues, M. Vilanova, A. Benito, A human ribonuclease induces apoptosis associated with p21WAF1/CIP1 induction and JNK inactivation, BMC Cancer 11 (2011) 1–12.